Empirical Analysis of Near-Fault Forward-Directivity Effects in the 2010-11 Canterbury Earthquakes

V.A. Joshi & B.A. Bradley

Department of Civil and Natural Resources Engineering, University of Canterbury, Christchurch.

2013 NZSEE Conference

ABSTRACT: In this paper, the characteristics of near-fault ground motions recorded during the M_w7.1 Darfield and M_w 6.2 Christchurch earthquakes are examined and compared with existing empirical models. The characteristics of forward-directivity effects are first examined using a wavelet-based pulse-classification algorithm. This is followed by an assessment of the adequacy of empirical models which aim to capture the effect of directivity effects on amplifying the acceleration response spectra; and the period and peak velocity of the forward-directivity pulse. It is illustrated that broadband directivity models developed by Somerville et al. (1997) and Abrahamson (2000) generally under-predict the observed amplification of response spectral ordinates at longer vibration periods. In contrast, a recently developed narrowband model by Shahi and Baker (2011) provides significantly improved predictions by amplifying the response spectra within a small range of periods surrounding the directivity pulse period. Although the empirical predictions of the pulse period are generally favourable for the Christchurch earthquake, the observations from the Darfield earthquake are significantly under-predicted. The elongation in observed pulse periods is inferred as being a result of the soft sedimentary soils of the Canterbury basin. However, empirical predictions of the observed peak velocity associated with the directivity pulse are generally adequate for both events.

1 INTRODUCTION

Near-fault strong ground motions resulting from the M_w 7.1 Darfield (4 September, 2010) and M_w 6.2 Christchurch (22 February, 2011) earthquakes were well recorded by the dense set of strong motion instrumentation installed in Christchurch city and the surrounding Canterbury Plains. Recent studies by Bradley (2012) and Bradley and Cubrinovski (2011) have identified the presence of forward-directivity effects in the near-fault ground motions resulting from the Canterbury earthquakes. This phenomenon occurs due to the alignment of the rupture front and direction of slip along the causative fault towards a given site. The occurrence of forward-directivity is highlighted by the presence of a large long period pulse in the velocity time-series, which is observed at the beginning of the record, and represents the cumulative effect of almost all of the seismic radiation from the fault (Somerville et al., 1997). This pulse is typically observed in the fault-normal component of the velocity time-series due to the constructive interference of shear waves propagating towards a site.

Figure 1 illustrates the observed velocity time-series at Rolleston (ROLC) and Pages Road (PRPC) during the Darfield and Christchurch earthquakes, respectively. Evidence of forward-directivity is clearly demonstrated by the pulse (shown in blue) arriving at the beginning of the fault-normal velocity-time series. At both sites, the observed peak ground velocities (PGV) in the fault-normal direction (approximately 108cm/s and 95cm/s, respectively) are large in relation to the fault-parallel direction (approximately 67cm/s and 38cm/s, respectively). Due to the short duration and large amplitude of this pulse, which consequently places large demands on structures, the incorporation of forward-directivity effects in seismic design is extremely important.

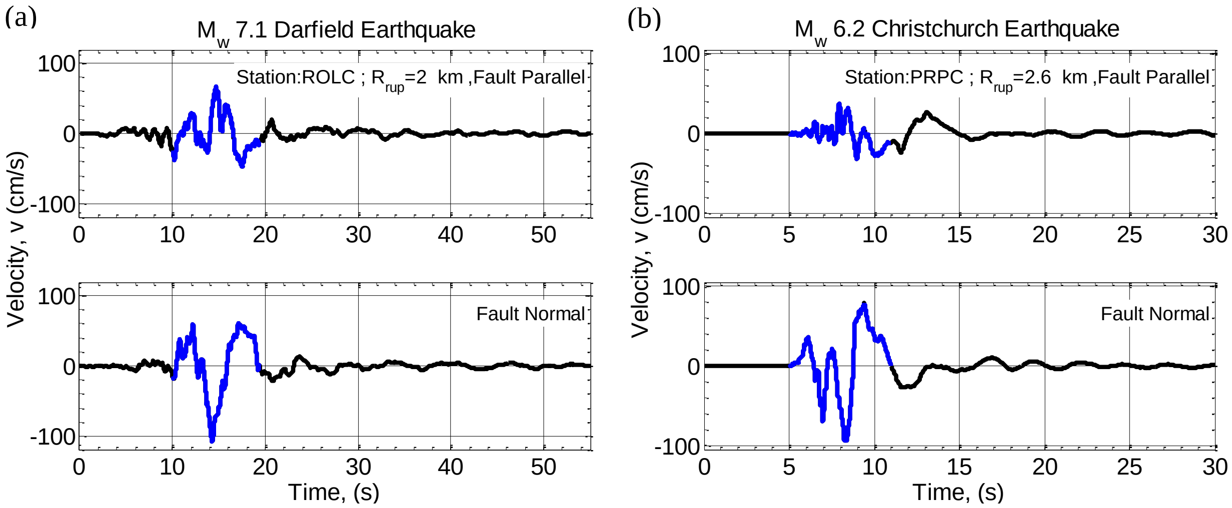

Figure 1: Evidence of strong forward-directivity effects in the fault-normal velocity time-series recorded at (a) Rolleston (ROLC) during the Mw 7.1 Darfield earthquake; and (b) Pages Road (PRPC) during the Mw 6.2 Christchurch earthquake.

In this paper, ground motions from the Canterbury earthquakes exhibiting forward-directivity are firstly identified using a wavelet-based pulse classification algorithm. Secondly, the adequacy of several existing models for prediction of: (i) amplification of the response spectrum; and (ii) predominant period (T_p) and peak ground velocity (PGV) of the velocity pulse are assessed using these observations. Finally, using the latest NGA (Next Generation Attenuation)-West 2 pulse-type ground motion database, empirical equations are developed for the estimation of the directivity pulse period and amplitude in an effort to determine whether improved predictions can be obtained based on recent datasets.

2 CHARACTERISTICS OF OBSERVED FORWARD-DIRECTIVITY EFFECTS IN THE CANTERBURY EARTHQUAKES

Previous documentation of observed forward-directivity in near-fault ground motions recorded during the Canterbury earthquakes (Bradley 2012 & Bradley & Cubrinovski 2011) has been based on qualitative visual evidence, i.e. the presence of a pulse-like feature in the fault-normal velocity time-series as well as the preferred direction taken by the velocity trajectory plot. In order to assist in quantification of forward-directivity effects, Baker (2007) developed an automated pulse classification algorithm which identifies pulse-like ground motions. The algorithm utilises wavelet analysis to extract the main pulse-like feature from a given component of the velocity time-series. A pulse indicator score, indicating the likelihood that a ground motion record is pulse-like, is calculated based on the PGV and energy (represented by the cumulative squared velocity) associated with the residual record (extracted pulse subtracted from the original ground motion) and the original record (Baker 2007). A high score ($\geq$0.85) indicates a pulse-like record whereas a score of 0.15 or less indicates a non-pulse like record. The period of the extracted pulse is defined as the period at which the maximum Fourier amplitude is reached. In order to determine whether the ground motion is pulse-like potentially due to forward-directivity effects, Baker (2007) proposed the following two additional criteria: (i) the PGV of the ground motion record must be greater than 30cm/s; and (ii) the pulse must arrive early in the velocity time-series, as indicated by the criterion developed using the cumulative squared velocity of the extracted pulse and original record.

In order to highlight the use of the Baker (2007) algorithm, the near-fault ground motion recorded at the Templeton (TPLC) strong motion station (SMS) during the Darfield earthquake is used as an example. Figure 2a shows the use of the algorithm in extracting the pulse-like feature from the original fault-normal velocity time-series. It is important to note that the original time-series is characterised by an initial forward-directivity pulse followed by several cycles of large amplitude and long period ground motion due to basin-induced surface wave effects (Bradley, 2012). It can be seen that the algorithm is unable to capture the initial directivity pulse and selects the second predominant cycle of ground motion associated with basin-generated surface waves. In order to overcome this limitation, a cut-off is manually applied in the original velocity time-series at approximately 18s (shown by the solid blue line in Figure 2b). In this manner, the algorithm is forced to extract the principal directivity pulse and the ground motion is classified as pulse-like for physically-appropriate reasons. Thus, this example illustrates that additional criteria maybe required in the Baker (2007) algorithm in order to ensure that significant basin-induced surface waves are not incorrectly extracted.

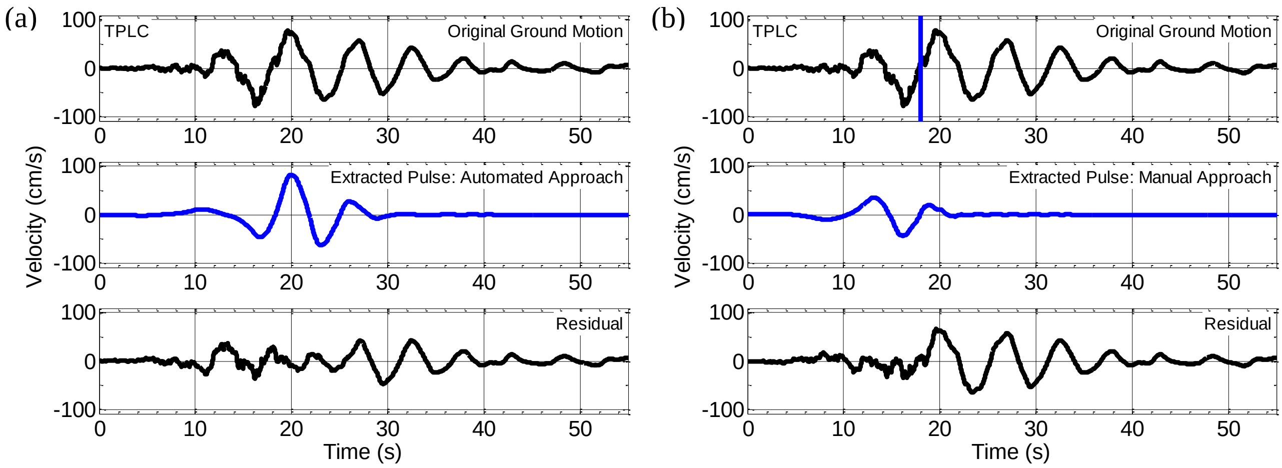

Figure 2: Baker (2007) wavelet analysis algorithm applied to the ground motion recorded at Templeton (TPLC) during the Darfield earthquake using (a) automated; and (b) manual approaches.

Tables 1 and 2 provide a summary of the results associated with the wavelet analysis performed on the near-fault ground motions observed in the Darfield and Christchurch earthquakes, respectively. In some cases, as highlighted in Tables 1 and 2, the pulse indicator scores suggest that the ground motions are potentially non pulse-like. However, based on visual examination of the records and source-to-site geometry, it was concluded that these ground motions show clear evidence of forward-directivity effects.

Table 1: Forward-directivity ground motions identified using the wavelet-analysis algorithm in the M_w 7.1 Darfield earthquake.

Station ID[1]	PGV (cm/s)	Pulse Period, Tp (s)	Pulse Indicator Score	Late Arrival	Pulse-Like Motion
CACS	33.4	8.3	0.98	No	Yes [2]
CBGS	62.0	5.7	1	No	Yes [2]
CCCC	74.2	3.5	0.83	No	Yes [3]
CHHC	70.6	3.7	0.12	No	Yes [3]
CMHS	42.2	3.0	0.05	No	Yes [3]
DSLC	54.3	8.1	1	No	Yes [2]
GDLC	118.9	5.1	0	No	Yes [3]
HORC	83.1	2.2	1	No	Yes [2]
HPSC	50.2	3.8	1	No	Yes [2]
LINC	109.1	7.2	1	No	Yes [2]
NNBS	48.3	6.9	0.72	No	Yes [3]
PPHS	72.9	8.0	0.58	No	Yes [3]
PRPC	64.6	3.8	1	No	Yes [2]
REHS	68.2	4.2	1	No	Yes [2]
RHSC	56.3	4.6	1	No	Yes [2]
ROLC	107.9	7.2	1	No	Yes [2]
SHLC	58.2	7.2	0.75	No	Yes [3]
SMTC	41.3	3.8	1	No	Yes [2]

TPLC	77.4	7.2	1	No	Yes [2]

[1] Refer to Bradley (2012) and Bradley & Cubrinovski (2011) for details on SMS locations.

[2] As determined by the classification criteria proposed by Baker (2007).

[3] Classified as pulse-like based on visual examination of the record and source-to-site geometry, although the pulse indicator scores suggest otherwise.

Table 2: Forward-directivity ground motions identified using the wavelet-analysis algorithm in the M_w 6.2 Christchurch earthquake.

Station ID[1]	PGV (cm/s)	Pulse Period, Tp (s)	Pulse Indicator Score	Late Arrival	Pulse-Like Motion
CBGS	67.2	1.8	1.00	No	Yes [2]
CCCC	69.5	1.4	1.00	No	Yes [2]
CHHC	72.6	3.7	0.97	No	Yes [2]
CMHS	45.6	1.7	1.00	No	Yes [2]
HVSC	91.0	0.5	1	Yes	Yes [3]
LPCC	50.5	3.2	0.97	No	Yes [2]
LPOC	81.9	1.7	1.00	No	Yes [2]
PPHS	36.4	3.8	1.00	No	Yes [2]
PRPC	98.7	3.9	0.99	No	Yes [2]
REHS	97.9	1.6	0.99	No	Yes [2]
RHSC	37.8	3.9	1.00	No	Yes [2]
SHLC	55.9	1.2	1.00	No	Yes [2]

[1] Refer to Bradley (2012) and Bradley & Cubrinovski (2011) for details on SMS locations.

[2] As determined by the classification criteria proposed by Baker (2007).

[3] Classified as pulse-like based on visual examination of the record and source-to-site geometry, although the wavelet-analysis algorithm suggests otherwise due to the late arrival of the pulse.

It should be noted that directivity effects were significant in the Darfield earthquake and were observed primarily in the fault-normal component of the velocity time-series. The significance of directivity can be explained by the size of the event (M_w 7.1), strike-slip faulting mechanism and rupture propagation of the central and eastern section of the Greendale fault toward Christchurch (Holden et al. 2011, Bradley 2012). In contrast, according to Bradley & Cubrinovski (2011), forward-directivity effects from the Christchurch earthquake were only prevalent over a smaller area in the eastern suburbs of Christchurch due to the misalignment between the direction of slip and inferred direction of rupture propagation on the causative reverse thrust fault. In the present study, the near-fault ground motions from the Christchurch event were rotated through all possible non-redundant orientations in order to detect the presence of pulse-like features. In general, it was found that the effects of rupture directivity in ground motions from the Christchurch earthquake were evident in orientations similar to the fault-parallel direction, although a smaller number of ground motions exhibited this phenomenon in comparison with the Darfield event.

The result that pulse-like ground motion characteristics were prevalent in orientations nearly fault parallel based on the one-fault model of Beavan et al. (2011) can possibly be explained by a subsequently developed fault-slip model by Beavan et al. (2012), which indicates a segmented rupture process involving three different fault planes. The occurrence of directivity pulses in orientations other than the inferred fault-normal orientation have also previously been documented in reverse-faulting events such as the 1994 Northridge earthquake, which is likely further illustration of the uncertainty in finite fault models, and the subsequent determination of the fault-normal direction (Wald et al. 1996, Howard et al. 2005).

3 ASSESSMENT OF RESPONSE SPECTRUM AMPLIFICATION DUE TO FORWARD-DIRECTIVITY

Conventional ground motion prediction equations (GMPE) (e.g. Bradley 2010) generally do not account for the observed effects of rupture directivity on elastic pseudo-acceleration response spectral amplitudes (SA). There are two general types of empirical models which modify the predicted response spectral amplitudes due to this near-source phenomenon, and are referred to as 'broadband' and 'narrowband' models. Somerville et al. (1997) developed the first broadband model, which monotonically increases, or decreases, the average horizontal spectral ordinates over a broad range of periods, beginning at T=0.6s. Based on empirical evidence from the 1999 Chi-Chi and Kocaeli earthquakes, Somerville (2003) confirmed that the directivity pulse is however 'narrowband' in nature, with a pulse period that increases with earthquake magnitude (M_w). As a consequence, it was found that the corresponding response spectra demonstrate peaks centred about the pulse period. More recently, Shahi & Baker (2011) developed the first comprehensive narrowband model based on empirical calibration of pulse-like ground motions from the NGA strong ground motion library. In particular, they proposed a function for the amplification of average horizontal SA predicted by a GMPE for a range of periods centred about the pulse period.

The present study focuses on assessing the adequacy of the broadband and narrowband models using observed forward-directivity ground motions from the Canterbury earthquakes. Figure 3 illustrates the observed average horizontal response spectra at Christchurch Hospital in the Darfield earthquake, compared to the prediction of the Bradley (2010) GMPE (shown in blue). An amplification of the observed spectral ordinates in the region surrounding the pulse period (T_p= 3.7s) is clearly visible. Figures 3a and 3b also illustrate the directivity amplification predicted by the Somerville et al. (1997) and Shahi & Baker (2011) models (hereafter referred to as S97 and SB11 respectively). The inset of the figures display the calculated geometric parameters (obtained using the finite fault model developed by Holden et al. (2011)) and pulse period (obtained using the Baker (2007) wavelet analysis algorithm), respectively. It is evident from Figure 3a that the observed forward-directivity amplification is significantly under-predicted by the S97 model. Conversely, the SB11 narrowband amplification in Figure 3b provides an accurate prediction of the observed amplification consistent with theoretical considerations.

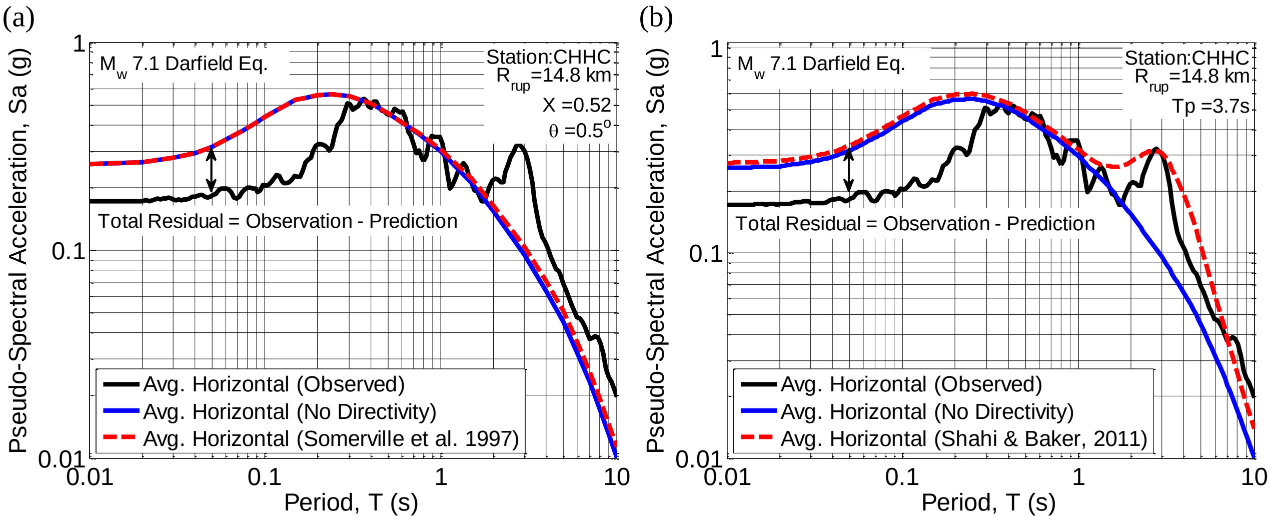

Figure 3: Amplification of the response spectra due to forward-directivity effects predicted by (a) Somerville et al. (1997) broadband model; and (b) Shahi and Baker (2011) narrowband model for Christchurch Hospital (CHHC) in the Mw 7.1 Darfield earthquake.

The total residuals, which represent the difference between the observed and predicted SA values normalised by the total standard deviation of the GMPE, and therefore an indication of bias, were computed for all forward-directivity ground motions in the Darfield and Christchurch earthquakes.

Figures 4a and 4b show the mean value of all of the total residuals as a function of the vibration period for the Darfield and Christchurch events, respectively. A value of $\varepsilon_{mean} = 0$ indicates no bias whereas a value of $\varepsilon_{mean} = 1$ indicates that the observations are one standard deviation above the median prediction on average. It should be noted that 'BR10' corresponds to the Bradley (2010) GMPE without any modification for forward-directivity and 'AB00' corresponds to the Abrahamson (2000) broadband directivity amplification model, which is a modified version of the S97 model for strike-slip events. Figure 4a illustrates that that the use of a conventional GMPE without any directivity amplification results in notable under-prediction ($\varepsilon_{mean} > 0.5$) of spectral ordinates at longer vibration periods (T>4s) for the Darfield event. In the Christchurch event, neglecting the directivity amplification results in smaller under-prediction as illustrated in Figure 4b. The results of Figure 4a and 4b also illustrate that upon adjusting the median prediction of the BR10 GMPE using the S97 directivity model, the observed amplification remains significantly under-predicted, which can be attributed to the inherent 'broadband' nature of the model. In fact, the model predicts a deamplification of spectral ordinates at longer vibration periods for several sites in the Christchurch event, thereby resulting in a slightly larger under-prediction in comparison to the BR10 GMPE predictions in Figure 4b. In contrast, using the AB00 model for the Darfield event results in a notable reduction of the mean residuals in relation to the S97 model, with ε_{mean} ranging between -0.6 and 0.6. A further reduction in mean residuals can be seen for the Darfield and Christchurch events using the SB11 narrowband amplification model as illustrated in Figures 4a and 4b, respectively. For example, the model significantly over-predicts the observed amplification between vibration periods of T=1s and T=5s for both events, with ε_{mean} less than -0.5 in this period range. In addition, it is important to note the fact that forward-directivity effects are accounted for in the NZ design code response spectra by the near-fault factor (NZS1170.5 2004), which is based on the S97 broadband model. The inadequacy of this factor has been highlighted in previous studies (e.g. Bradley 2012) and has been further exemplified in this study, albeit in an indirect manner.

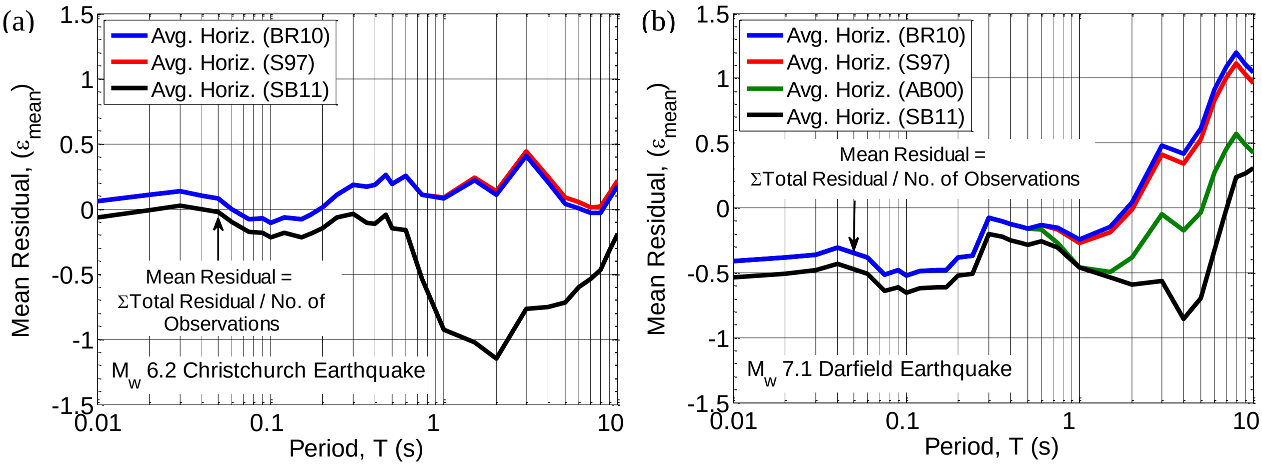

Figure 4: Mean residuals associated with the broadband and narrowband model predictions for (a) M_w 7.1 Darfield; and (b) M_w 6.2 Christchurch earthquakes.

In order to further emphasise the adequacy of the narrowband response spectral amplification model, Figure 5 compares the mean amplification (i.e. the ratio of spectral ordinates corresponding to the original ground motion and residual ground motion from the wavelet analysis) demonstrated by the forward-directivity ground motions in the Canterbury earthquakes to the empirical model of SB11, as a function of the normalised vibration period. The amplification associated with the individual ground motions is also shown by the thin grey lines. As expected, the observed mean amplification functions form a bell-shaped pattern with peaks close to $T/T_p = 1$, thereby highlighting the narrowband nature of the directivity pulse. It can be seen that, on average, the amplification resulting from forward-directivity in both events is lower than that predicted by the SB11 model.

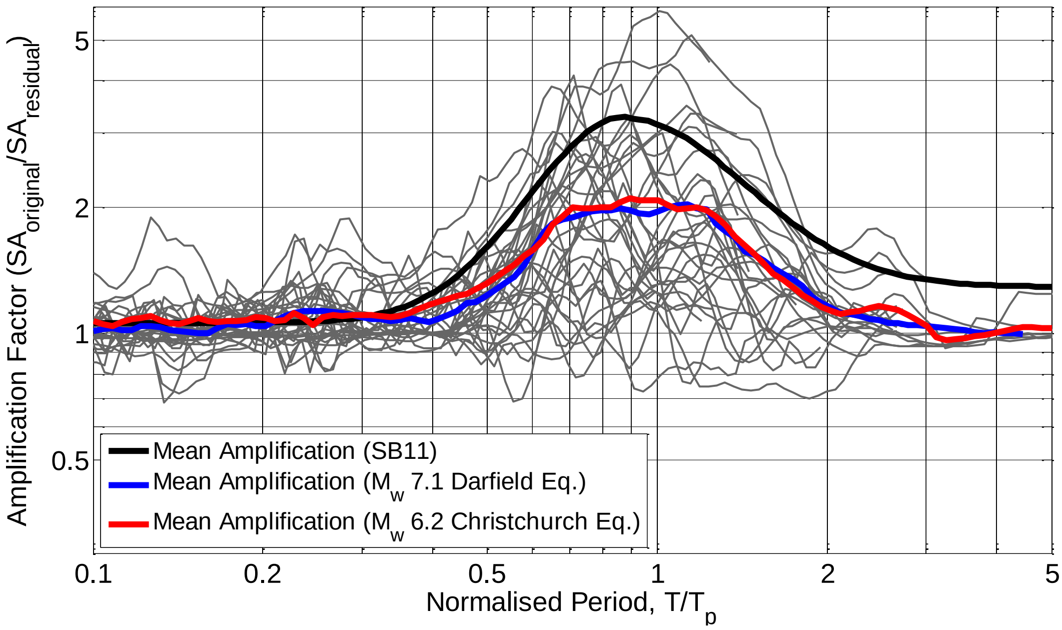

Figure 5: Comparison of the mean amplification of spectral ordinates observed in forward-directivity ground motions of the Canterbury earthquakes with the empirical amplification of the Shahi and Baker (2011) narrowband model.

4 ASSESSMENT OF EMPIRICAL MODELS FOR PERIOD AND PEAK VELOCITY OF THE FORWARD-DIRECVITY PULSE

Previous research (e.g. Alavi & Krawlinker 2000) has found that the nonlinear structural response of structures in the near-fault region is particularly sensitive to the amplitude and period of the velocity pulse. Based on these findings, several researchers have focussed their efforts on developing predictive relationships for these parameters. The observations from the recent Canterbury earthquakes (refer to Tables 1 and 2) are used here to determine the adequacy of these models.

4.1 Pulse Period

Figures 6a and 6b illustrate the empirical CDFs corresponding to observed pulse period in the Darfield and Christchurch events, respectively, compared to the prediction of several empirical relationships. It is important to note that Bray & Rodriguez-Marek (2004) and Bray et al. (2009) employ the same definition of the pulse period (i.e. visual measurement from the velocity time-series) except that the latter study included a larger database of ground motions. Shahi & Baker (2011) developed their empirical relationship based on the pulse periods obtained as part of identifying pulse-like ground motions from the NGA database using the Baker (2007) wavelet analysis algorithm.

It is clear from the CDFs in Figure 6a that the observed median pulse period of T_p = 5.1s in the Darfield event is significantly greater than that predicted by empirical equations (which give median pulse periods of 2.7s, 2.5s, 3.7s and 3.4s, respectively). On the other hand, the observed median T_p = 1.8s in the Christchurch event compares more favourably with the empirical predictions (which give median pulse periods of 1.2s, 1.4s, 1.5s and 1.4s, respectively) in Figure 6b, however, it can be seen that the empirical distribution is still notably further ‘right’ than the prediction CDFs. Empirical evidence from previous earthquakes (e.g. the 1989 M_w 7.0 Loma Prieta earthquake) has consistently shown that pulse periods from forward-directivity ground motions recorded on soil sites are higher in relation to rock sites due to the effects of local site response. This has been further illustrated analytically by seismic site response analyses using forward-directivity ground motions (Bray & Rodriguez-Marek 2006). Hence the observed elongation in pulse period could be attributed to the influence of soft sedimentary soils underlying a majority of Christchurch.

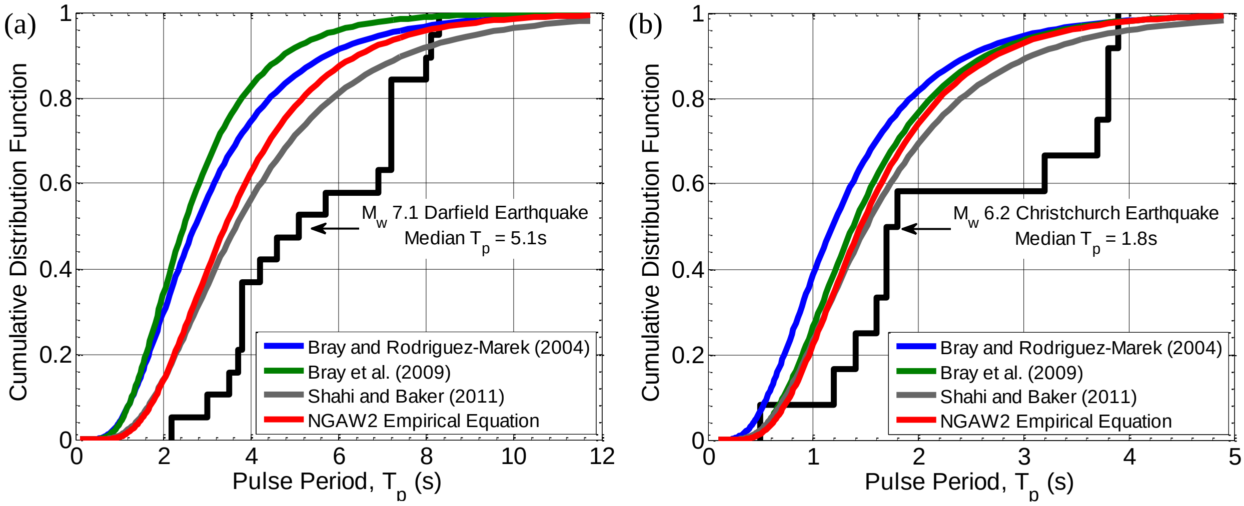

Figure 6: Comparison of the cumulative distribution functions associated with observed directivity pulse periods from (a) Mw 7.1 Darfield; and (b) Mw 6.2 Christchurch earthquakes with empirical prediction equations.

The aforementioned three pulse period models are based on a deprecated NGA ground motion database. In order to assess whether more recent data provide an improved comparison with the Canterbury earthquake observations, 222 pulse-like ground motions from the latest NGAW2 database were used to determine an empirical relationship for T_p, as shown by equation (1):

$$\ln (T_p)_{ij} = -5.53 + 0.95M_w + \eta_i + \varepsilon_{ij} \; ; \sigma_{total} = 0.49; \sigma = 0.36; \tau = 0.33 \qquad (1)$$

where $(T_p)_{ij}$ is the pulse period of the j^{th} ground motion from the i^{th} event; M_w is the moment magnitude of event i; η_i is the inter-event term (with standard deviation, $\tau = 0.33$); and ε_{ij} intra-event term (with standard deviation, $\sigma = 0.36$). It is worth noting that a modified version of the Baker (2007) wavelet analysis algorithm was used in characterising the period of the pulses (Shahi & Baker pers. comm. 2012) in the NGAW2 database. The lognormal CDF associated with this model (NGAW2 empirical equation) is also shown in Figures 7(a) and 7(b) for the Darfield and Christchurch events, respectively. It can be observed that the predictions are very similar to the more recent SB11 model for both events, thereby highlighting the fact that the use of an up-to-date larger database does not result in improved predictions of the pulse periods from these events, and therefore highlighting the importance of region-specific features on directivity characteristics.

4.2 **Pulse Amplitude**

The peak ground velocity (PGV) has been identified as an effective measure of the directivity pulse amplitude in previous research. Figures 7a and 7b illustrate the observed peak velocities in the forward-directivity ground motions of the Darfield and Christchurch events, respectively. For comparison, the median predictions (50^{th} percentile) of several empirical relationships are also shown as a function of source-to-site distance (R_{rup}). It should be noted that the Bray and Rodriguez-Marek (2004) and Bray et al. (2009) equations (hereafter referred to as BR04 and BR09, respectively) were developed for the near-fault region (R_{rup}< 20km), whereas the Chiou & Youngs (2008) equation (hereafter referred to as CY08) is a conventional GMPE developed using a large database of near-fault and far-fault ground motions.

A large majority of the observed pulse-like ground motions in the Darfield event are at distances greater than 10km, as shown in Figure 8(a). In contrast, the observations from the Christchurch event in Figure 8(b) lie between distances of 1km and 10km. The results of both figures indicate that the BR04, CY08 and BR09 models are able to accurately predict the observed peak velocities between source-to-site distances of 1km and 10km. However, at larger distances, these models predict larger attenuation of the pulse amplitude, thereby resulting in an under-prediction of the observed PGV values which becomes significant for R_{rup} > 15km.

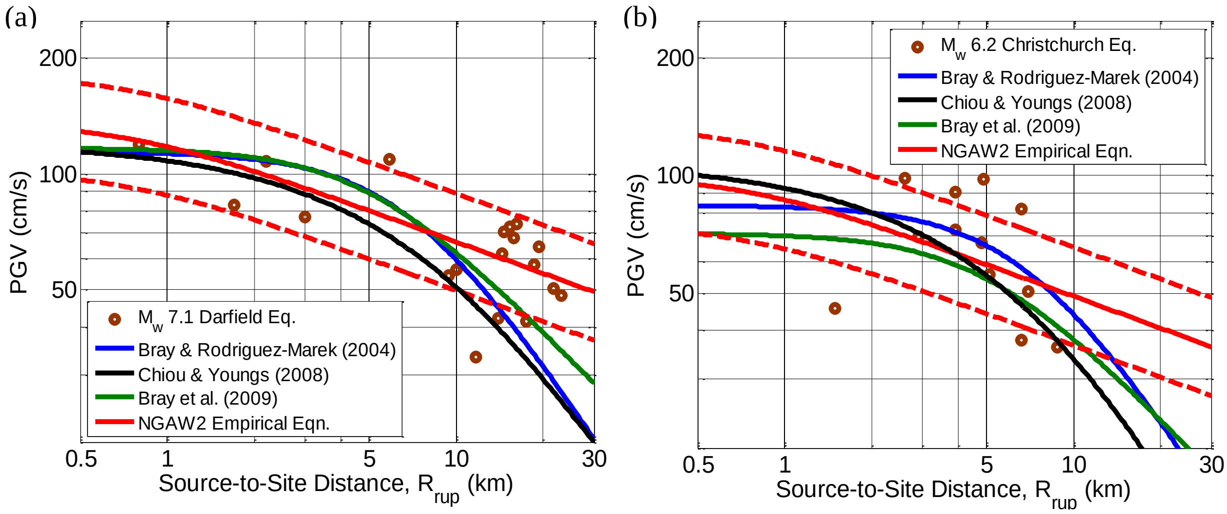

Figure 7: Comparison of observed values of PGV in forward-directivity ground motions from (a) Mw 7.1 Darfield earthquake; and (b) Mw 6.2 Christchurch earthquake with median predictions from empirical equations. The dotted red lines represent the 16th and 84th percentiles associated with NGAW2 model predictions.

Similar to that for pulse period, in this study, the simple functional form used by Bray & Rodriguez-Marek (2004) and Bray et al. (2009) was adopted in developing an empirical prediction equation using 111 near-fault pulse-like ground motions from the NGAW2 database to examine the differences in model prediction based on a current dataset. The relationship obtained using mixed-effects regression is shown by equation (2):

$$\ln(PGV)_{ij} = 2.83 + 0.30M_w - 0.18\ \ln(R_{rup}^2 + 0.74^2) + \eta_i + \varepsilon_{ij} \qquad (2)$$

$\sigma_{total} = 0.33$; $\sigma = 0.29$; $\tau = 0.16$

where $(PGV)_{ij}$ is the PGV (in cm/s) of the j^{th} ground motion from the i^{th} event; M_w is the moment magnitude of event i; R_{rup} is the closest distance from the fault plane to the site; η_i is the inter-event term (with standard deviation, $\tau = 0.16$); and ε_{ij} is the intra-event term (with standard deviation, $\sigma = 0.29$). The median predictions associated with this model (NGAW2 empirical equation) are shown for both events in Figures 8(a) and (b) along with the 16^{th} and 84^{th} percentiles, as illustrated by the dotted red lines. It can be seen that the model provides similar predictions of PGV between source-to-site distances of 1km and 10km to the BR04, CY08 and BR09 models. However, the attenuation of pulse amplitudes at larger distances (R_{rup} > 15km) occurs more gradually in relation to the other models, thereby providing better estimates of the observed peak velocities in the Darfield earthquake.

5 CONCLUSIONS

The near-fault ground motions recorded in the M_w 7.1 Darfield and M_w 6.2 Christchurch earthquakes show clear evidence of forward-directivity effects. A wavelet-based pulse classification algorithm was used to identify and document ground motions exhibiting this damaging near-source phenomenon. In the Darfield event, the principal directivity pulse was observed in the inferred fault-normal orientation, which is consistent with the rupture propagation along the central and eastern segments of the predominantly strike-slip Greendale fault towards Christchurch. In contrast, several near-fault ground motions from the Christchurch event contained velocity pulses in orientations similar to the inferred fault-parallel direction, possibly due to a complex rupture process involving multiple fault segments, as suggested by a subsequently developed fault-slip model.

The adequacy of empirical models, which aim capture the effect of forward-directivity on pseudo-acceleration response spectra, were subsequently assessed using ground motions observed in the Canterbury earthquakes. It was found that broadband models, which form the basis of the near-fault factor in the NZS1170.5:2004, did not provide accurate predictions of the observed forward-directivity amplification of longer period spectral ordinates. The amplification predicted by a recently developed model of Shahi & Baker (2011), which accounts for the 'narrowband' nature of the directivity pulse, provides an improved prediction, but was higher than the observed amplification. The results of these comparisons indicate that changes to the near-fault factor can be achieved by the incorporation of the more appropriate narrowband models in seismic hazard analyses that form the basis of design response spectra.

The efficacy of empirical prediction models for the vibration period and amplitude (i.e. peak ground velocity, PGV) of the directivity pulses observed in the Canterbury earthquakes were also examined. Although comparisons between observed and predicted pulse periods for the Christchurch event were favourable, significant under predictions resulted for the Darfield event. The empirical equations for PGV generally provided accurate predictions in comparison to observations from the Canterbury earthquakes for source-to-site distances between 1km and 10km, but under-predicted the PGV amplitudes at greater distances. A simple model for PGV, developed based on near-source ground motions in the most recent NGA-West2 database provides a more appropriate attenuation of PGV with distance and does not exhibit such bias.

REFERENCES

Abrahamson, N. A. (2000). Effects of rupture directivity on probabilistic seismic hazard analysis. *Proceedings of the 6th Internation Conference on Seismic Zonation.* Palm Springs.

Alavi, B., & Krawlinker, H. (2000). Consideration of Near-Fault Ground Motion Effects in Seismic Design. *12th World Conference in Earthquake Engineering.* Auckland.

Baker, J. W. (2007). Quantitative Classification of Near-Fault Ground Motions using Wavelet Analysis. *Bulletin of the Seismological Society of America , 97* (5), 1486-1501.

Beavan, J., Fielding, E., Motagh, M., Samsonov, S., & Donnelly, N. (2011). Fault Location and Slip Distribution of the 22 February 2011 Mw 6.2 Christchurch, New Zealand Earthquake from Geodetic Data. *Seismological Research Letters , 82* (6).

Beavan, J., Motagh, M., Fielding, E., Donnelly, N., & Collett, D. (2012). Fault slip models of the 2010–2011 Canterbury, New Zealand, earthquakes from geodetic data and observations of post-seismic ground deformation. *New Zealand Journal of Geology and Geophysics , 55* (3), 207-221.

Bradley, B. A. (2010). *NZ-specific pseudo-acceleration ground motion prediction equations based on foreign models.* Research Report No.2010-03, University of Cantebury, Department of Civil and Natural Resources Engineering, Christchurch.

Bradley, B. A. (2012). Strong ground motion characteristics observed in the 4 September 2010 Darfield, New Zealand earthquake. *Soil Dynamics and Earthquake Engineering , 42*, 32-46.

Bradley, B. A., & Cubrinovski, M. (2011). Near-source Ground Motions Observed in the 22 February 2011 Christchurch Earthquake. *Seismological Research Letters , 82* (6), 853-865.

Bray, J. D., & Rodriguez-Marek, A. (2004). Characterization of the forward-directivity ground motions in the near-fault region. *Soil Dynamics and Earthquake Engineering , 24*, 815-828.

Bray, J. D., Rodriguez-Marek, A., & Gillie, J. L. (2009). Design Ground Motions Near Active Faults. *Bulletin of the New Zealand Society for Earthquake Engineering* .

Chiou, B. S.-J., & Youngs, R. R. (2008). An NGA Model for the Average Horizontal Component of Peak Ground Motion and Response Spectra. *Earthquake Spectra , 24* (1), 173-215.

Holden, C., Beaven, J., Fry, B., Reyners, M., Ristau, J., Van Dissen, R., et al. (2011). Preliminary source model of the Mw7.1 Darfield earthquake from geological, geodetic, and seismic data. *9th Pacific Conference on Earthquake Engineering.* Auckland.

Howard, J. K., Tracy, C. A., & Burns, R. G. (2005). Comparing Observed and Predicted Directivity in Near-Source Ground Motion. *Earthquake Spectra , 21* (4), 1063-1092.

NZS1170.5. (2004). *Structural Design Actions, Part 5: Earthquake Actions- New Zealand.* Wellington.

Rodriguez-Marek, A., & Bray, J. D. (2006). Seismic Site Response for Near-Fault Forward Directivity Ground Motions. *Journal of Geotechnical and Geoenvironmental Engineering* .

Shahi, S. K., & Baker, J. W. (2011). An Empirically Calibrated Framework for Including the Effects of Near-Fault Directivity in Probabilistic Seismic Hazard Analysis. *Bulletin of the Seismological Society of America , 101* (2), 742-755.

Somerville, P. G. (1998). Development of An Improved Representation of Near-Fault Ground Motions. *Seminar on Utilisation of Strong-Ground Motion Data*, (pp. 1-20). Oakland.

Somerville, P. G. (2003). Magnitude scaling of the near fault rupture directivity pulse. *Physics of the Earth and Planetary Interiors , 137* (1-4), 201-212.

Somerville, P. G., Smith, N. F., Graves, R. W., & Abrahamson, N. A. (1997). Modification of Empirical Strong Ground Motion Attenuation Relations to Include the Amplitude and Duration Effects of Rupture Directivity. *Seismological Research Letters , 68* (1), 199-222.